Mechanism of selective gold extraction from multi-metal chloride solutions by electrodeposition-redox replacement†

Ivan Korolev, [ID] [a,b] Stylianos Spathariotis, [ID] [c] Kirsi Yliniemi, [ID] [d] Benjamin P. Wilson, [ID] [a] Andrew P. Abbott [ID] [c] and Mari Lundström [ID] *[a]

The electrodeposition-redox replacement (EDRR) process is a promising method for a selective extraction of minor metals from complex mixtures. When it is performed in a benign medium (such as sodium chloride solution or deep eutectic solvent), the EDRR method provides a non-toxic alternative for a conventional cyanide-based process. The detailed reaction mechanisms of the EDRR in Cu–Au systems, as well as the effect of the reaction medium are elucidated in this article. Electrogravimetric studies show that the EDRR process comprises three distinct stages: (1) deposition of Cu at a constant applied potential; (2) dissolution of deposited Cu at open circuit conditions in reaction with dissolved species in solution; (3) reduction of Au to elemental form in reaction with various Cu species. It is discovered that the recovery of Au takes place surprisingly *via* both the redox replacement between Cu and Au at the surface and the homogeneous Au reduction by Cu(ɪ) species in solution. Both of these reaction pathways are facilitated by open circuit conditions (redox replacement step) between electrodeposition cycles and the utilization of other sacrificial elements in the solution is crucial. The use of aqueous chloride solution is advantageous over 1:2 ChCl:EG for the increased Au recovery (94.4%) and the purity of the product (93.7%), although it consumes slightly more electricity. Therefore, the EDRR enables energy and resource efficient selective extraction of Au from multi-metal industrial solutions even when it is present at low concentrations.

Introduction

The global focus on the sustainable use of Earth's natural resources, especially non-renewables like metals and minerals, demands that the concepts of circular economy be realized on an industrial scale.[1,2] The use of raw materials – both primary and secondary – must be performed with low energy and chemical consumption, and with minimum waste accumulation.[3,4] At the same time, the renewable energy has become more affordable and easily available making electrochemical metal recovery methods a feasible option to reduce the carbon footprint of extractive industry.[5,6] With this

framework in mind, the electrodeposition-redox replacement (EDRR) method has been introduced for selective recovery of gold,[7,8] silver,[9,10] and platinum[11] from complex industrial effluents. It has also been studied for its versatility and ability to create functional surfaces directly from industrial process solutions.[12,13] Nevertheless, the process mechanism is currently only understood on a phenomenological level and more detailed investigations into the reactions involved has not been carried out yet. In this paper, the underlying mechanism of the gold recovery from copper containing solutions – including both aqueous and deep eutectic solvents – by EDRR is explored for the first time. Such an in-depth understanding is essential when it comes to the exploitation of EDRR's full potential, the main goal being the sustainable recovery of gold from solutions which contain precious metals only in trace amounts and other base metals (*e.g.*, copper) as major elements.

Following the principles of green engineering,[14] sustainable gold production also encourages the development of eco-friendly, non-toxic extractants to replace commonly used cyanide.[15,16] Chloride-based processes of gold leaching have proven their efficiency and are considered a viable alternative to conventional hydrometallurgical technologies.[17,18] The

[a]*Hydrometallurgy and Corrosion, Department of Chemical and Metallurgical Engineering, Aalto University, 02150 Espoo, Finland. E-mail: mari.lundstrom@aalto.fi*
[b]*Outotec Research Center, 28101 Pori, Finland*
[c]*Materials Centre, Department of Chemistry, University of Leicester, LE1 7RH, UK*
[d]*Department of Chemistry and Material Science, Aalto University, 02150 Espoo, Finland*

efficient extraction of gold in aqueous chloride solutions is possible even with minor reagent addition.[19] However, in some regions of the world, water is viewed as a critical resource, and reducing its consumption is one of key requirements for a sustainable development.[20,21] Among non-aqueous lixiviants, the environmentally benign deep eutectic solvents (DESs) are the subject of significant research from a metallurgical perspective.[22–24] Their wide electrochemical window makes DESs especially advantageous in deposition and plating applications for metals with low reduction potential, such as aluminum, chromium, zinc and nickel.[25–27] In addition, DESs enable precious metals to be oxidized at lower overpotentials,[28] and are thus preferred in leaching applications.[29–32]

In this paper, the effects of solvent's physicochemical properties, such as metal speciation and mass transport, on the efficiency of the EDRR method were investigated in aqueous chloride solution and in deep eutectic mixture of choline chloride with ethylene glycol in $1:2$ molar ratio ($1:2$ ChCl : EG). Moreover, the concentration of chloride ions in this DES is *ca.* 4.8 M, which is similar to commonly used in hydrometallurgical gold recovery processes,[33–36] and therefore it makes the comparative study of these two systems from the EDRR perspective justified.

Experimental

Chemicals

The aqueous solution was prepared by mixing AuCl, $CuCl_2 \cdot 2H_2O$ and NaCl in deionized water to obtain the following concentrations: 5×10^{-4} M Au, 6×10^{-2} M Cu and 4.5 M Cl^-. HCl was added to maintain pH below 3. This Cu : Au ratio of $120:1$ was selected based on previous investigations that simulated gold chloride leaching solutions.[7] DES solution was made by mixing choline chloride $(CH_3)_3NC_2H_4OHCl$ (ChCl) with 1,2-ethanediol $HOCH_2CH_2OH$ (EG) in a molar ratio of $1:2$ and then gold and copper chloride salts were added in order to obtain the same concentrations as present in the aqueous solution. All chemicals were of reagent grade (Sigma Aldrich, USA). The concentration of dissolved oxygen was measured in both chloride-containing solutions prior to experiments with a Clark-type polarographic sensor and it was 1.56 mg l^{-1} in aqueous 4.5 M NaCl solution and 1.32 mg l^{-1} in $1:2$ ChCl : EG.

Electrodeposition-redox replacement method

The EDRR method – previously described in more detail[7] – includes two consecutive stages that are repeated N times:

• electrodeposition (ED) stage – the potentiostatic deposition of copper at potential E_{dep} for a short time t_{ED};
• redox replacement (RR) stage – when the system is switched to open circuit conditions for a time t_{RR} to allow redox replacement between gold and copper.

Actual values of the EDRR process parameters E_{dep}, t_{ED}, t_{RR} are dependent on the solution composition and for aqueous solution, the parameters were based on previous research.[7] For

Table 1 Process parameters for the EDRR experiments

Solution	E_{dep} (V *vs.* Ag/AgCl)	t_{ED} (s)	t_{RR} (s)	N
Aqueous 4.5 M NaCl	−0.35	10	600	50
1 : 2 ChCl : EG	−0.45			

$1:2$ ChCl : EG solution, the E_{dep} value can be identified from the copper deposition range in cyclic voltammetry (CV), while t_{ED} and t_{RR} are kept the same as for the aqueous solution (Table 1).

Electrochemical quartz-crystal microbalance experiments

EQCM experiments were performed in a three-electrode cell with the Gamry eQCM 10 MHz resonator controlled by a Reference 600 potentiostat (Gamry Instruments, USA). A 10 MHz platinum coated AT-cut quartz crystal (surface area: 0.21 cm^2) was used as a working electrode and platinum foil as a counter electrode (area: 3 cm^2). The measurements in aqueous solutions were conducted with the standard Ag/AgCl (sat. KCl) reference electrode (0.197 V *vs.* SHE, SI Analytics, Germany), whereas in non-aqueous the reference electrode consisted of a silver wire immersed in a 0.1 M solution of AgCl in $1:2$ ChCl : EG and separated from the electrochemical cell by a Vycor glass frit to allow for the mobility of the ions. For the consistency of reporting, all the potential values in the figures and text are brought to the same basis following the procedure described by Frenzel *et al.*[37] and referred *vs.* Ag/AgCl.

According to the Sauerbrey equation,[38] a frequency shift Δf of the quartz crystal is proportional to the mass change Δm on the electrode:

$$\Delta f = -C_f \cdot \Delta m \quad (1)$$

For an AT-cut 10 MHz quartz crystal with an active surface area of 0.21 cm^2, the constant equals $C_f = 1.1$ Hz ng^{-1}. On the other hand, assuming that only faradaic processes occur during the deposition, the mass recovered on the electrode can be related to the amount of charge Q passed during deposition time t_{ED} through Faraday's law:

$$\Delta m = \frac{QM}{zF} \quad (2)$$

where M is the molar mass of the deposit, z is number of electrons and $F = 96\,485$ C mol^{-1} is the Faraday constant. Combining eqn (1) and (2), the ratio M/z can be calculated:

$$\frac{M}{z} = -\frac{\Delta f}{Q} \cdot \frac{F}{C_f} \quad (3)$$

Rotating ring-disk electrode measurements

Rotating ring-disk electrode (RRDE) measurements were performed with a variable speed set-up (MSR, Pine Research, US): the platinum disk (area: 16.4 mm^2) mounted in Teflon was surrounded by a platinum ring (3.6 mm^2) with a 180 µm gap

between them, resulting in the set-up of two working electrodes, hereafter referred to as a disk electrode and a ring electrode. The counter electrode was a platinum mesh and reference electrode Ag/AgCl (0.197 V *vs.* SHE, SI Analytics, Germany). The disk electrode was held at −0.35 V *vs.* Ag/AgCl for 1 min before the potential was set to $E_D = 0.1$ V *vs.* Ag/AgCl. At the same time the amperometric measurement was started at the ring electrode with constant oxidizing potential $E_R = 0.65$ V *vs.* Ag/AgCl. Apparent collection efficiency N_{app} of the RRDE is the ratio of the current at the ring i_R to the current at the disk electrode i_D:

$$N_{app} = -\frac{i_R}{i_D} \times 100\% \qquad (4)$$

Process efficiency evaluation

The composition and morphology of the surface were analyzed with a Zeiss Sigma 300 scanning electron microscope (SEM) equipped with an EDX detector (Carl Zeiss Ltd, UK). The applied acceleration voltage and the beam intensity were 5 kV and 0.2 nA, respectively. Metal recoveries were calculated from the inductively coupled plasma mass-spectroscopy (iCAP Q, Thermo Scientific, USA) assays of the solutions before and after the EDRR experiments. As the potential was applied to the cell only during the deposition step, the specific energy consumption w, kW h kg^{-1}, can be calculated as follows:

$$w = \frac{Q \cdot E_{cell}}{3600 \cdot m_{Au}} \qquad (5)$$

where E_{cell} is the cell voltage between working and counter electrodes, and m_{Au} is the mass of recovered gold.

Results and discussion

Speciation of gold and copper in chloride solutions

Cyclic voltammograms (CV) recorded in both aqueous 4.5 M NaCl and 1 : 2 ChCl : EG solutions containing 60 mM Cu and 0.5 mM Au display similar features (Fig. 1a), *i.e.* reduction and oxidation peaks of copper and gold, although their positions are slightly shifted. Lower cathodic limit of stability exists in the 1 : 2 ChCl : EG solution around −1.2 V *vs.* Ag/AgCl, while hydrogen evolution onset in the aqueous solution occurs already at −0.6 V *vs.* Ag/AgCl, providing the stability limit of this solution.

In the case of EDRR, the difference between the reduction potentials of the sacrificial metal, *e.g.* copper, and the metal being recovered, *i.e.* gold is an important parameter, affecting the overall efficiency of the process.[7] In theory, the further apart these two potentials are (and assuming no other steps or species), the bigger the driving force is for the redox replacement reaction.[39] However, the lower the reduction potential of the sacrificial metal, the higher are the cell voltage and energy consumption for the deposition. Therefore, all of these potentials affect greatly the efficiency of EDRR. Fig. 1a shows that in both solutions the potential difference between copper and gold reduction peaks is nearly the same, about 0.85 V *vs.* Ag/AgCl, albeit their positions in 1 : 2 ChCl : EG have moved in a cathodic direction, and the cupric/cuprous reaction is partially overlapping with the gold reduction peak. The absolute values of open circuit potential (OCP) are different in two systems (0.51 V *vs.* Ag/AgCl in 1 : 2 ChCl : EG against 0.69 V *vs.* Ag/AgCl in aqueous solution), but in both cases it falls in the region where copper(ii) and gold(i) species are the dominant species in the solution.

The speciation of copper and gold in aqueous chloride solutions has been extensively researched in past decades,[40–42] and it was found that the prevailing copper chlorocomplexes in 4.5
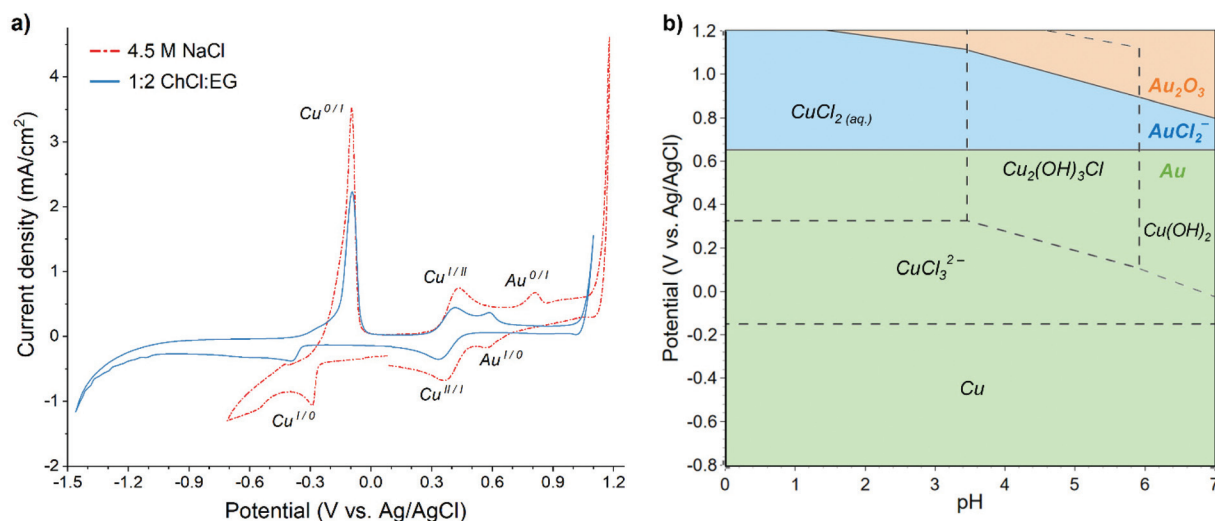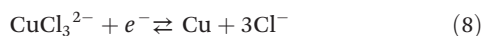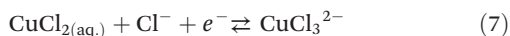

Fig. 1 (a) Cyclic voltammogram of 60 mM Cu + 0.5 mM Au in aqueous 4.5 M NaCl and 1 : 2 ChCl : EG solutions, scan rate 20 mV s^{-1}. (b) Pourbaix diagram for aqueous Au−Cu−Cl system at 25 °C ([Au] = 0.5 mM, [Cu] = 60 mM, [Cl] = 4.5 M), generated in HSC Chemistry 10 software.

M NaCl brine are $CuCl_2^0$ and $CuCl_3^{2-}$, whereas gold is mostly present as $AuCl_2^-$. The predominance regions of these species are illustrated in the Pourbaix diagram (Fig. 1b) and it corroborates the assignment of electrochemical processes to the peaks seen in the voltammogram, which could thus be expressed by following half-reactions:

$$AuCl_2^- + e^- \rightleftarrows Au + 2Cl^- \tag{6}$$

$$CuCl_{2(aq.)} + Cl^- + e^- \rightleftarrows CuCl_3^{2-} \tag{7}$$

$$CuCl_3^{2-} + e^- \rightleftarrows Cu + 3Cl^- \tag{8}$$

Although the chloride content in $1:2$ ChCl:EG is similar to that of aqueous 4.5 M NaCl solution, the speciation of metals differs due to lower concentration of available water ligands.[43] The dominant species in this case are $CuCl_4^{2-}$ and $AuCl_2^-$, along with $CuCl_2^-$ for monovalent copper.[44–46] Therefore, the reactions according to eqn (6) as well as eqn (9) and (10) can be associated to the corresponding peaks in $1:2$ ChCl:EG solution:

$$CuCl_4^{2-} + e^- \rightleftarrows CuCl_2^- + 2Cl^- \tag{9}$$

$$CuCl_2^- + e^- \rightleftarrows Cu + 2Cl^- \tag{10}$$
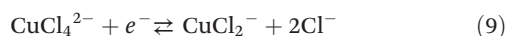
Electrogravimetric study

The electrochemical quartz crystal microbalance (EQCM) is a powerful tool to study both faradaic and gravimetric aspects of electrochemical reactions simultaneously, and it is often used to study metal deposition and dissolution processes.[47–49] Theoretical background of the method is comprehensively described in the literature[50–52] that makes it a technique of choice for studying the recovery of gold by the EDRR process.

In total, 50 cycles of EDRR were carried in both solutions (Fig. 2) and it shows a clear pattern of the EDRR process. During ED there was a rapid increase in the deposited mass. This was followed by a RR step, showing first a sharp decline and then a moderate growth of the mass. During 50 cycles the trend shows a clearly increasing change in mass with an average rate around 9.7 µg cm^{-2} h^{-1} in the aqueous solution. A smaller total mass change was observed in $1:2$ ChCl:EG, with two different rates for mass increase; the average deposition rate dropped from 5.4 µg cm^{-2} h^{-1} at the start of the measurement to 2.4 µg cm^{-2} h^{-1} by the end of the experiment. This is most likely due to the higher viscosity and lower ionic conductivity of the DES that causes slower mass transport.[53] Despite this difference, during the RR stage, a mass increase was observed in both systems, retarding only slightly with the number of cycles.

Magnification of one EDRR cycle in Fig. 2 shows that it consists of three consecutive electrochemical processes:

• metal deposition during the ED stage resulting in a significant surge in mass over a short period of time;

• rapid stripping of metal from the electrode surface as soon as the potential is switched off and the cell is at open circuit potential conditions (start of RR step);
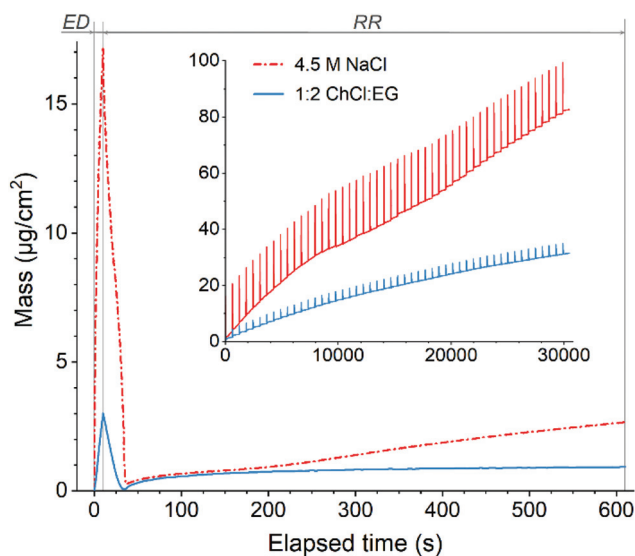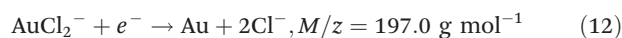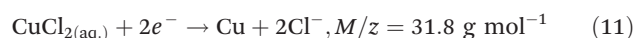

Fig. 2 Variation of mass during one EDRR cycle (10 s ED + 600 s RR) in aqueous 4.5 M NaCl solution and $1:2$ ChCl:EG (60 mM Cu, 0.5 mM Au, T = 25 °C). Inset: mass change throughout 50 EDRR cycles.

• gradual mass buildup on the electrode *via* different redox reactions during the rest of RR stage.

In order to understand this behavior, each of these events was examined to get the full picture of the reaction mechanism of the EDRR process.

Metal deposition during ED stage. The value of M/z (mass deposited by 1 mol of electrons) is a useful parameter when identifying the electrode processes and examining their respective efficiencies,[54–56] as it indicates whether only one or several electrochemical processes occur simultaneously at the electrode surface; this is done by comparing the observed M/z ratio to the value calculated for a single electrochemical reaction. A good agreement between the observed and theoretical M/z values suggests that the proposed reaction is prevailing, whereas differences indicate that other mechanisms can be taking place in parallel, *e.g.* redox reactions in the solution, adsorption and desorption of species on the electrode surface, changes in double layer structure, and liquid entrapment into a rough deposit.[57,58]

The M/z values obtained for ED from aqueous solution (Fig. 3a) in all cycles exceed the theoretical value for copper deposition – denoted with a dotted line – according to eqn (11), suggesting that more than one reaction take place simultaneously. The most likely parallel reaction in absence of other metals is a co-deposition of gold according to eqn (12):

$$CuCl_{2(aq.)} + 2e^- \rightarrow Cu + 2Cl^-, M/z = 31.8 \text{ g mol}^{-1} \tag{11}$$

$$AuCl_2^- + e^- \rightarrow Au + 2Cl^-, M/z = 197.0 \text{ g mol}^{-1} \tag{12}$$

Because the OCP of both solutions lay below the oxidation potential of gold and hence cannot cause its dissolution, the extent of gold co-deposition could be approximated from the difference between mass deposited during ED and mass dis-
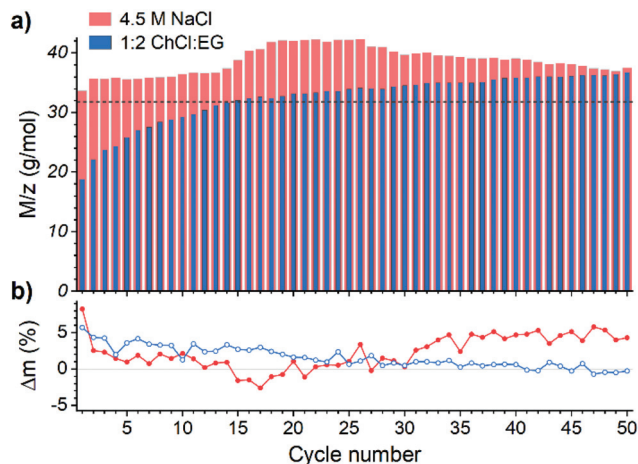
Fig. 3 (a) M/z value for the deposit obtained during the ED stage of each EDRR cycle. (b) Estimated co-deposition of gold from aqueous 4.5 M NaCl (red ●) or 1 : 2 ChCl : EG (blue ○) solution with 60 mM Cu and 0.5 mM Au.

solved in the RR step (Fig. 3b), assuming complete copper dissolution during the RR step. In both systems the average amount of co-deposited gold is about 2 wt%, which correlates well with the composition of the initial solution.

In aqueous solution, the gold co-deposition rate is roughly constant through the first 10–15 cycles as is the M/z ratio with an exception for the very first cycle, when the deposition occurs on the pristine Pt surface. Negative mass change observed in some cycles implies that more material was dissolved than deposited during that cycle, presumably due to "refining" of the gold accumulated on the electrode surface, *i.e.* dissolution of the residual copper that was entrained in the previous cycles. As the EDRR proceeds over 20 cycles, the difference between mass deposited and mass dissolved tends to increase (Fig. 3b), whereas the M/z shows the opposite trend; this is an indication of a declining faradaic efficiency of the electrodeposition caused by additional, undetermined side process(es), for example, nanoparticles adsorption onto the electrode surface and their further growth *via* nucleation or Ostwald ripening.[59,60]

While in the aqueous solution the M/z ratio is constantly above the theoretical line, in 1 : 2 ChCl : EG it evolves from 18.7 g mol^{-1} in the 1st cycle up to 36.7 g mol^{-1} in 50th cycle. In the early cycles rather low values are detected, due to decreased deposition efficiency as also non-faradaic processes occur at the solution–electrode interface, like double layer rearrangement and displacement of solvent molecules,[61,62] along with reactions according to eqn (12) and (13):

$$CuCl_4{}^{2-} + 2e^- \rightarrow Cu + 4Cl^-, M/z = 31.8 \text{ g mol}^{-1} \quad (13)$$
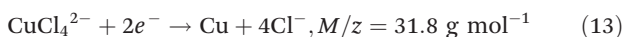
As the EDRR cycling continues, the local concentration of copper species in the proximity of the electrode rises due to a slow diffusion rate in 1 : 2 ChCl : EG. This leads to a lower gold co-deposition rate (Fig. 3b), but the concurrent increase of M/z suggests that reduction of cuprous species at the electrode

(eqn (10), $M/z = 63.5$ g mol^{-1}) starts playing a bigger role in the ED.

Stripping of the deposit at the start of RR stage. Fig. 4 shows magnifications of the first minutes of EDRR cycles, when the deposited copper rapidly dissolves in absence of the applied potential. Taking into account the composition of the studied solutions, possible drivers for copper dissolution are:

• redox replacement by dissolved gold;
• reaction with dissolved oxygen in the solution;
• oxidation to copper(ı) by dissolved cupric ions.

Although the redox replacement reaction (eqn (14)) is thermodynamically favored, this reaction is surface limited and therefore, only copper in the top-most surface layer will be replaced by gold:

$$Cu + AuCl_2{}^- + Cl^- \rightarrow Au + CuCl_3{}^{2-} \quad (14)$$

Moreover, redox replacement will not only dissolve copper from the surface but also deposit gold on the surface, thus the net mass change should be positive as gold is heavier than copper. However, the mass increase at the beginning of RR stage (Fig. 4c and d) is marginal, hence another mechanism of copper dissolution is prevailing.

The presence of Cl$^-$ ions in the solution alters the speciation of copper and makes possible its dissolution by cupric species. This can be deduced from the mass decrease of a copper-coated QCM crystal placed in different chloride containing media (Table 2). Minor amount of dissolved oxygen present in the solution under atmospheric conditions facilitates the oxidation of metallic copper,[63] further promoted by complexation with chloride ions.

The copper dissolution rate in the EDRR experiments (on average *ca.* 2700 μg cm^{-2} h^{-1}) was close to that observed in acidic copper-bearing aqueous 4.5 M NaCl solution (Table 2). Therefore, it can be concluded that the mass drop occurring in the aqueous solution in the beginning of the RR stage is caused by the oxidation of copper:

$$2Cu + CuCl_{2(aq.)} + 4Cl^- \rightarrow 2CuCl_3{}^{2-} \quad (15)$$
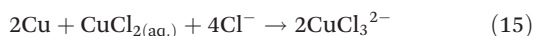
The redox potential of the aqueous solution measured during the RR (Fig. 4a) indicates a two-step electrochemical process. First, a dissolution of elemental copper according to eqn (15) happens at the potential around −0.2 V. This reaction is limited by the amount of copper on the electrode surface, which is corroborated by the mass change of the QCM crystal

Table 2 The dissolution rate of deposited copper in different chloride solutions

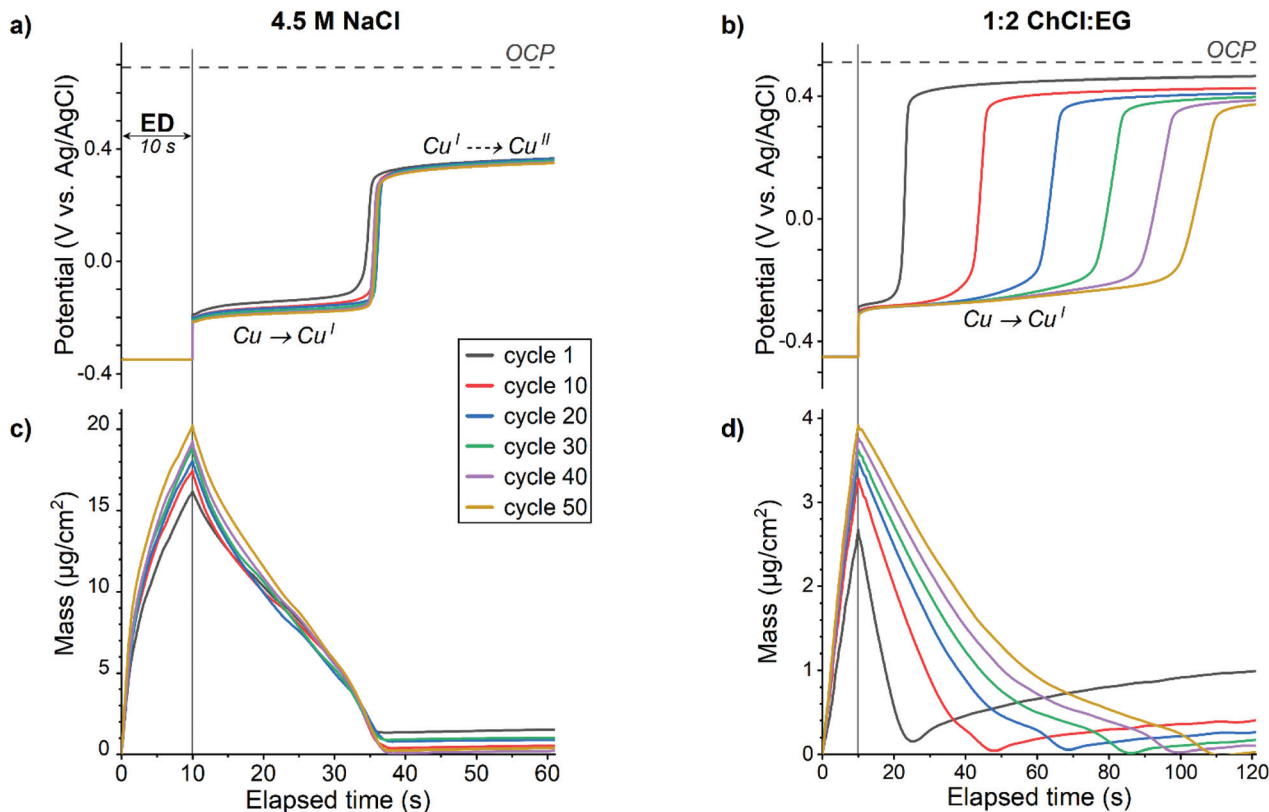| Solution	Dissolution rate (μg cm^{-2} h^{-1})
60 mM CuCl$_2$ (1 : 2 ChCl : EG)	2.5
60 mM CuCl$_2$ (aqueous)	119.9
10 mM HCl (aqueous)	201.2
60 mM CuCl$_2$ + 10 mM HCl (aqueous)	954.4
60 mM CuCl$_2$ + 10 mM HCl + 4.5 M NaCl (aqueous)	3289.0

Fig. 4 Measured potential (a, b) and mass change (c, d) during first minutes of EDRR cycles in aqueous 4.5 M NaCl solution (left) and in 1 : 2 ChCl : EG (right).

(Fig. 4c) – as soon as almost all of copper is stripped, the potential instantly shifts to a more positive direction. Thanks to a rapid mass transfer in aqueous solution, the dissolution time is rather constant in all 50 cycles and it takes about 25 s before the redox potential of the solution rises to *ca.* 0.3 V *vs.* Ag/AgCl. According to a CV (Fig. 1a), this potential corresponds to the cuprous/cupric redox reaction (eqn (7)) and implies that concentration of the copper(II) species increases in the vicinity of the electrode. Possible cathodic half-reactions are discussed below. The diffusion of oxidized species towards the electrode surface leads to a gradual rise of measured potential with time; however, due to changing with every EDRR cycle both the electrode surface and the composition of the solution, the initial OCP of 0.69 V *vs.* Ag/AgCl will not be reached.

In the 1 : 2 ChCl : EG solution, comproportionation reaction (eqn (16)) provides a plausible explanation for the oxidation of copper at the early RR stage in 1 : 2 ChCl : EG:[64,65]

$$Cu + CuCl_4^{2-} \rightarrow 2CuCl_2^{-} \quad (16)$$

The stability of the copper(I) complex in 1 : 2 ChCl : EG together with a slightly lower dissolved oxygen concentration and hindered mass transport leads to a gradual depletion of copper(II) species near the electrode with every cycle. As a result, the copper dissolution is slowed down by an order of magnitude (from 10 s to 100 s) as the EDRR progresses (Fig. 4d).

Mass accumulation during the RR step. The mass increase in the later stages of RR is attributed to the gold recovery. Naturally, some redox replacement will contribute but typically it takes place only on the surface layers and cannot fully explain the high increase of mass observed during the RR step. Therefore, an additional mechanism for gold recovery and constant mass increase needs to be explored.

The potential used in the EDRR (−0.35 V *vs.* Ag/AgCl) is by design[7] selected such that hydrogen evolution does not occur, so the reduction of gold by hydrogen is prevented. This was also verified by an additional EDRR experiment which was performed without copper in solution but using the same ED potential. The mass change during the EDRR cycles is shown in Fig. S1 in the ESI.† In RR step no mass gain were observed, which means that copper plays a crucial role in mass accumulation. It was previously reported[66,67] that under certain conditions cuprous ions may cause homogenous reduction of dissolved gold to its metallic state (eqn (17)), which provides a conceivable reason for such constant increase of mass on the electrode in addition to cementation:

$$AuCl_2^{-} + CuCl_3^{2-} \rightarrow Au + CuCl_{2(aq.)} + 3Cl^{-} \quad (17)$$

It is worth noting that if copper in aqueous solution is present only as its monovalent chlorocomplex, steady gold

mass buildup begins even without any potential applied to the electrode.[67] This was experimentally demonstrated in a measurement, where copper(I) chloride was added to solution instead of copper(II) chloride salt (Fig. S2†). Also, the mass increase is observed at the deposition rate of 19.6 μg cm^{-2} h^{-1}, which is more than double of the rate measured in a copper(II) solution due to increased amount of cuprous ions available. This finding emphasizes the essential function of copper(I) ions for the recovery of gold from the aqueous solution, and the fact that in EDRR copper(I) can be generated electrochemically – rather than through chemical addition – highlights the versatility of this method. Moreover, previous research has shown that cuprous species are more stable in concentrated chloride media when compared to dilute solutions, both in aqueous systems[68,69] and in deep eutectic solvents,[70,71] which can further promote the role of copper(I) in gold recovery.

Electrogravimetric measurements alone, however, cannot conclusively interpret the mechanism in details, and RRDE amperometry is often used to define the reaction paths and determine the rates of competing chemical reactions.[72,73] Additional generator–collector experiments with RRDE were performed in aqueous chloride solution for definitive verification of the role of copper(I) complexes in the gold recovery process (Fig. S3†).

The disk electrode, after a short copper deposition period, was set to the copper dissolution potential (0.1 V *vs.* Ag/AgCl) while the ring was constantly maintained at the copper(I)/copper(II) oxidation potential (0.65 V *vs.* Ag/AgCl), so that anodic current observed on the ring electrode indicates the cuprous/cupric reaction. Apparent collection efficiency (Fig. 5) of the ring electrode is smaller than the theoretical efficiency ($N = 21.8\%$) either with or without gold in solution, and this suggests that a parallel chemical reaction, which does not involve gold, is consuming copper(I) species. In copper chloride solution, this could be due to oxidation of copper(I) to copper(II):

$$CuCl_3{}^{2-} + \frac{1}{4}O_2 + H^+ \rightarrow CuCl_{2(aq.)} + Cl^- + \frac{1}{2}H_2O \quad (18)$$
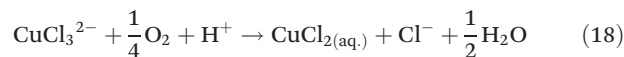
In the presence of gold in the solution, the apparent collection efficiency is approximately 30% lower, showing that cuprous ions are also consumed for the homogenous reduction of gold (eqn (17)). Further decrease in collection efficiency at faster rotation speed is related to a better aeration of the solution and much improved mass transfer of oxygen; more cuprous species are oxidized according to eqn (18) and hence are not detected at the ring electrode. Therefore, it can be concluded that both redox replacement at the electrode surface and reduction of gold by copper(I) species in solution volume are the reasons for the mass increase on the electrode during the RR step with the latter one being prevalent.

Process efficiency

The efficiency of the overall EDRR process was estimated through the amount of gold recovered from either the aqueous chloride solution or 1 : 2 ChCl : EG after 50 cycles of EDRR. The quality of the obtained product is also shown in the Table 3. A particularly high selectivity is achieved for gold recovery from the aqueous solution with the purity of the cathode product close to 95%. A small amount of oxygen was detected on the surface, which is most likely because of its oxidation in contact with air. The SEM micrographs (Fig. 6) highlight the difference in the quality of the obtained deposit. The EDRR process carried out in aqueous solution resulted in a granular morphology with fine gold particles (*ca.* 10 nm) distributed over the surface. These particles also appear to aggregate into larger clusters up to a few μm in size. Irregular surface coverage could be partly a result of the nanoparticle growth through coalescence and recrystallization of neighboring nuclei particles.[74,75]

In 1 : 2 ChCl : EG, on the other hand, the coating was smoother, though very uneven in chemical composition. The surface was covered with a thin film composed mostly of gold, but occasionally incorporating some amount of copper. Also, the EDX analysis of the deposit (Fig. S4†) showed significant levels for carbon as a result of solvent being trapped inside the deposit. Few micron-size gold particles occur sparingly across the surface as well, often surrounded by a halo of organic substances. Poor gold recovery from the 1 : 2 ChCl : EG in compari-
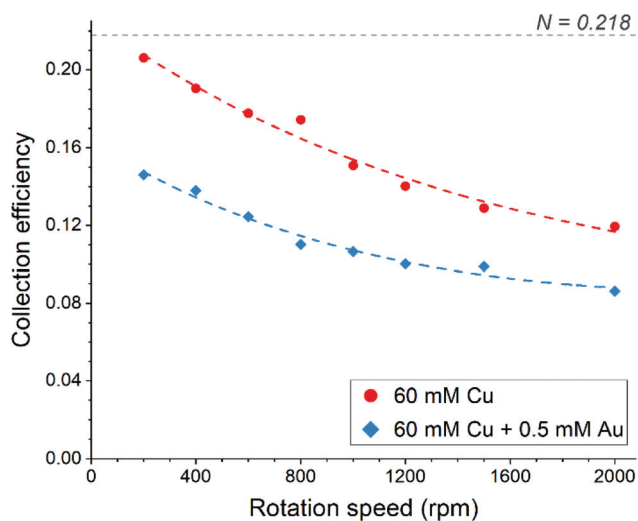

Fig. 5 Apparent collection efficiency of the ring-disk electrode as a function of rotation speed in aqueous 4.5 M NaCl solution.

Table 3 Metal recoveries and composition of the final deposit

Solution	Recovery, wt%		Content in the deposit[a], at%			
	Au	Cu	Au	Cu	O	C
4.5 M NaCl	94.4	0.10	93.7	1.4	5.0	—
1 : 2 ChCl : EG	13.9	0.18	22.5	2.3	9.2	66.1

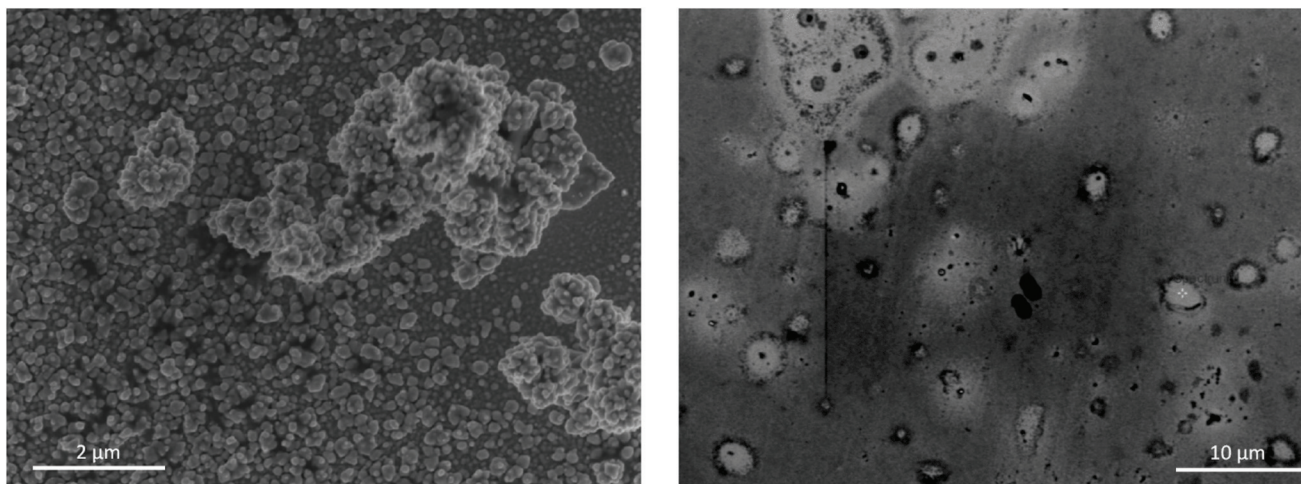[a] Excluding Pt background from working electrode.

Fig. 6   SEM images of electrode surface after 50 cycles of EDRR in aqueous 4.5 NaCl solution (left) and in 1 : 2 ChCl : EG (right).

son to aqueous solution is due to the mass transport limitations. The effect of restricted mass transport could be overcome by mixing or heating the solution. Nevertheless, the copper content in the final product obtained from both solutions is rather low at about 2 at%, implying effective gold enrichment and selective dissolution of copper during the RR step.

In conventional gold recovery processes, the purity of gold cathodes exceeds 99% with traces of other elements found only at a ppm level.[76,77] This is achieved by passing the leaching solution through a sophisticated process flowsheet that includes several concentration and purification operations, such as carbon adsorption/ion exchange and elution prior to electrochemical recovery by electrowinning.[78] By using EDRR instead, gold can be recovered in one stage directly from complex impure process solutions, with remarkable selectivity and acceptable purity for further refining to the bullion grade. The energy consumption is nearly the same in both cases, 11.6 kW h kg^{-1} in aqueous solution and 9.7 kW h kg^{-1} in 1 : 2 ChCl : EG, which falls in the range of the values achieved in the state-of-the-art industrial processes.[79,80] However, the higher gold recovery and purity of the product make the aqueous chloride solution preferable medium for the selective recovery of gold by EDRR process.

Discussion

Based on the results of EQCM study and RRDE measurements, the reaction mechanism of the EDRR process in aqueous chloride solution is outlined as follows:

• during the ED stage, copper is deposited at constant potential on the electrode together with a minor amount of co-deposited gold – eqn (11) and (12);

• when the current is switched off (early RR stage), the deposited copper starts to dissolve through the reaction with copper(II) species in the solution (eqn (15)), facilitated by low

pH, dissolved oxygen and high concentration of chlorides; also, the redox replacement reaction according to eqn (14) occurs on the surface to a certain extent;

• at the same time, gold is continuously reduced throughout the RR stage by the reaction with cuprous species (generated from the dissolution of deposited copper) in the vicinity of the electrode surface (eqn (17)) and precipitated onto the working electrode.

In 1 : 2 ChCl : EG, the process follows a similar route, although some of the reactions are different due to the distinct physicochemical properties of the solvent; for instance, the driving force of copper stripping (the presence of cupric ions in the vicinity of the electrode surface) and the hindered kinetics due to the poor ionic conductivity in 1 : 2 ChCl : EG. Therefore, gold recovery takes place *via* both the homogenous reduction in solution followed by precipitation and the redox replacement at the surface, and the open circuit conditions (RR stage) between electrodeposition steps is a necessity for both reaction pathways.

The role of fairly stable intermediate copper(I) species in the process investigated makes the copper–gold chloride system rather atypical from the EDRR perspective, and it is debatable as to whether such reaction processes should be referred to as EDRR rather than pulse electrodeposition followed by an open circuit potential step (ED-t_{OCP}). Indeed, the pure redox replacement action was reported for metal couples like platinum/lead,[81] platinum/nickel[82] or silver/zinc.[83] The common feature of these systems is that the sacrificial metal (either nickel, lead or zinc) can be present in the solution only in one oxidation state, *i.e.* "+2". As a consequence, when the sacrificial metal dissolves from the electrode surface, it does not form intermediate species, and therefore no reduction of valuable metal (silver or platinum) occurs in the solution volume. Other elements with similar behavior, such as tin, arsenic or bismuth were also shown suitable as sacrificial metals in EDRR process for recovery of valuable metals from hydrometallurgical process solutions.[84]

The copper(I) species involved in the homogenous reduction of dissolved gold are produced almost exclusively through dissolution of previously electrodeposited copper with a tiny fraction of cuprous chlorocomplexes also formed during short ED step by a one-electron reduction of copper(II) species (eqn (7)). The excessive charge applied to the system to reduce copper to its elemental state therefore seems to be "wasted", and the energy consumption of the overall gold recovery process is high. The energy efficiency might be improved by producing copper(I) at lower overpotential, *i.e.* without actual copper deposition. Also, the optimization of the RR time may further minimize the diffusion of copper(I) species out of the reaction layer, although consequently decreasing the local concentration of dissolved gold species. Nevertheless, the copper layer deposited on the electrode surface during the ED step is shown to make a contribution (however small it is) to ensuring the adhesion of gold nanoparticles to the substrate. In the studied copper–gold chloride system, the redox replacement cannot be totally excluded even if the major contribution of gold recovery arises from the dissolution of the electrodeposited copper as cuprous chlorocomplexes, followed by homogenous gold reduction in the liquid phase by the same copper(I) species. These results clearly highlight that the process, which involves a short deposition step followed by an extended time at OCP, results in a dramatic increase in the rate of gold extraction.

If there were no species in the intermediate oxidation state formed in the process, the homogenous reduction of gold in the solution would not occur, and thus only redox replacement at the solid/liquid interface would contribute to the gold recovery. This was observed in the 1 : 2 ChCl : EG solution, in which the copper(I) species are fairly stable and do not tend to oxidize further to cupric chlorocomplexes, hence the extent of homogenous reaction of dissolved gold with copper was minimal. Another way to ensure that redox replacement reaction prevails over precipitation is to use an alternative sacrificial metal that exists only in one oxidized state in the solution like silver, tin or bismuth. Unfortunately, in a majority of industrial applications it is not always possible to tailor the solution composition prior to the metal recovery since this is governed by the upstream processes.

From an industrial perspective, the EDRR process could be applied to recover gold from process streams that contain gold in minor amounts with respect to a base metal, like copper. Usually, such solutions result from the hydrometallurgical treatment of gold ores and concentrates,[85,86] recycling of electronic scrap,[87,88] leaching of anode slimes,[89,90] or refining of platinum group metals (PGM).[91,92] Depending on the origin, the solution will have various impurities that can influence the EDRR process. For example, effluents from PGM refineries contain residual amounts of dissolved platinum and palladium, which would reduce together with gold because of close values of standard electrode potential (0.755 V and 0.591 V for platinum(IV) and palladium(IV) chlorocomplexes, respectively).[93] Similar behavior is expected for other metals with standard reduction potentials that fall in the range between those of gold and copper, *e.g.* silver, antimony, arsenic. These metals will end up in the cathode product and potentially lower its purity. On the other hand, with skillful tailoring of the electrochemical parameters, these metals can act as the sacrificial elements for further recovery of the most noble element. This was previously suggested to occur in nickel-rich sulfate solution, as copper and nickel replacement was dominated by silver, but with increasing number of EDRR cycles platinum further replaced silver on the electrode surface.[11] Any elements that reduce at potentials more negative than copper do not have any detrimental impact on the EDRR process of gold recovery. However, special attention needs to be paid to iron, which is a typical impurity in ore leaching. In aqueous chloride solutions, iron – like copper – can be present in two oxidation states, either as di- or trivalent species. During the ED step of the EDRR process, iron(III) is reduced to iron(II), thus consuming some electric charge and decreasing the current efficiency.[83] In the RR step, the effect of iron is two-fold: ferric ions acting as an oxidant would enhance dissolution of the deposited copper and improve the purity of the gold deposit;[12] at the same time, ferrous ions may reduce dissolved gold in chloride media by a homogenous reaction, which increases overall recovery of gold from solution.[94]

Conclusions

Although the reaction pathway outlined is specific for the copper–gold chloride system investigated, this study reveals the crucial, beneficial roles of both the open circuit steps and other elements present in industrial solutions when it comes to metal recovery. Also, gold reduction in a solution does not exclude redox replacement reaction at the surface, but instead the possibility of both reaction routes increases the overall efficiency and can thus lead to a sustainable gold production from solutions containing only minor concentrations of a valuable metal. Both of these factors could – and should – be fully exploited in the extraction of other metals as they increase the efficiency without any additional chemical or energy consumption, which is in line with the green engineering principles. Overall, the EDRR process from aqueous solution appeared to be advantageous over deep eutectic solvent due to enhanced mass transfer and better-quality deposit. On the downside, a too rapid dissolution of copper at the start of the RR step may result in poor current efficiency and higher energy consumption. The power consumption of gold recovery achieved in this study was of the order of 10 kW h kg^{-1} from a solution containing only 0.5 mM Au, with the recovery efficiency of 95%, and this result is indeed a solid proof of the EDRR method's potential as an industrial gold extraction technology.

Conflicts of interest

There are no conflicts of interest to declare.

Acknowledgements

References

1 E. A. Olivetti and J. M. Cullen, *Science*, 2018, **360**, 1396–1398.

2 R. Bleischwitz, C. Spataru, S. D. VanDeveer, M. Obersteiner, E. van der Voet, C. Johnson, P. Andrews-Speed, T. Boersma, H. Hoff and D. P. van Vuuren, *Nat. Sustainability*, 2018, **1**, 737–743.

3 T. Keijer, V. Bakker and J. C. Slootweg, *Nat. Chem.*, 2019, **11**, 190–195.

4 M. A. Reuter, A. van Schaik, J. Gutzmer, N. Bartie and A. Abadías Llamas, *Annu. Rev. Mater. Res.*, 2019, **49**, 253–274.

5 B. C. McLellan, G. D. Corder, D. P. Giurco and K. N. Ishihara, *J. Cleaner Prod.*, 2012, **32**, 32–44.

6 O. Vidal, F. Rostom, C. François and G. Giraud, *Elements*, 2017, **13**, 319–324.

7 I. Korolev, P. Altinkaya, P. Halli, P.-M. Hannula, K. Yliniemi and M. Lundström, *J. Cleaner Prod.*, 2018, **186**, 840–850.

8 I. Korolev, E. Kolehmainen, M. Haapalainen, K. Yliniemi and M. Lundström, in *10th European Metallurgical Conference (EMC 2019)*, ed. U. Waschki, GDMB Verlag GmbH, Düsseldorf, Germany, 2019, vol. 2, pp. 623–630.

9 P. Halli, H. Elomaa, B. P. Wilson, K. Yliniemi and M. Lundström, *ACS Sustainable Chem. Eng.*, 2017, **5**, 10996–11004.

10 H. Elomaa, P. Halli, T. Sirviö, K. Yliniemi and M. Lundström, *Trans. IMF*, 2018, **96**, 253–257.

11 P. Halli, J. J. Heikkinen, H. Elomaa, B. P. Wilson, V. Jokinen, K. Yliniemi, S. Franssila and M. Lundström, *ACS Sustainable Chem. Eng.*, 2018, **6**, 14631–14640.

12 K. Yliniemi, Z. Wang, I. Korolev, P.-M. Hannula, P. Halli and M. Lundström, *ECS Trans.*, 2018, **85**, 59–67.

13 P.-M. Hannula, S. Pletincx, D. Janas, K. Yliniemi, A. Hubin and M. Lundström, *Surf. Coat. Technol.*, 2019, **374**, 305–316.

14 P. T. Anastas and J. B. Zimmerman, *Environ. Sci. Technol.*, 2003, **37**, 94A–101A.

15 G. Hilson and A. Monhemius, *J. Cleaner Prod.*, 2006, **14**, 1158.

16 J. Wang, Y. Lu and Z. Xu, *ACS Sustainable Chem. Eng.*, 2019, **7**, 7260–7267.

17 J. Viñals, E. Juan, M. C. Ruiz, E. Ferrando, M. Cruells, A. Roca and J. Casado, *Hydrometallurgy*, 2006, **81**, 142–151.

18 P. Altinkaya, J. Liipo, E. Kolehmainen, M. Haapalainen, M. Leikola and M. Lundström, *Min., Metall., Explor.*, 2019, **36**, 335–342.

19 R. Ahtiainen and M. Lundström, *J. Cleaner Prod.*, 2019, **234**, 9.

20 A. J. Gunson, B. Klein, M. Veiga and S. Dunbar, *J. Cleaner Prod.*, 2012, **21**, 71–82.

21 T. Sonderegger, S. Pfister and S. Hellweg, *Environ. Sci. Technol.*, 2015, **49**, 12315–12323.

22 Q. Zhang, K. de Oliveira Vigier, S. Royer and F. Jérôme, *Chem. Soc. Rev.*, 2012, **41**, 7108–7146.

23 E. L. Smith, A. P. Abbott and K. S. Ryder, *Chem. Rev.*, 2014, **114**, 11060–11082.

24 A. P. Abbott, R. C. Harris, F. Holyoak, G. Frisch, J. M. Hartley and G. R. T. Jenkin, *Green Chem.*, 2015, **17**, 2172–2179.

25 A. P. Abbott, G. Capper, K. J. McKenzie and K. S. Ryder, *J. Electroanal. Chem.*, 2007, **599**, 288–294.

26 A. P. Abbott, K. S. Ryder and U. König, *Trans. IMF*, 2008, **86**, 196–204.

27 V. S. Protsenko, L. S. Bobrova, D. E. Golubtsov, S. A. Korniy and F. I. Danilov, *Russ. J. Appl. Chem.*, 2018, **91**, 1106–1111.

28 A. P. Abbott, G. Frisch, S. Gurman, A. R. Hillman, J. Hartley, F. Holyoak and K. Ryder, *Chem. Commun.*, 2011, **47**, 10031–10033.

29 G. R. T. Jenkin, A. Z. M. Al-Bassam, R. C. Harris, A. P. Abbott, D. J. Smith, D. A. Holwell, R. J. Chapman and C. J. Stanley, *Miner. Eng.*, 2016, **87**, 18–24.

30 S. Anggara, F. Bevan, R. C. Harris, J. M. Hartley, G. Frisch, G. R. T. Jenkin and A. P. Abbott, *Green Chem.*, 2019, **21**, 6502–6512.

31 H. Elomaa, S. Seisko, J. Lehtola and M. Lundström, *J. Mater. Cycles Waste Manage.*, 2019, **21**, 1004–1013.

32 X. Li, W. Monnens, Z. Li, J. Fransaer and K. Binnemans, *Green Chem.*, 2020, **22**, 417–426.

33 D. Lu, L. Shi and Z. Jin, *Adv. Mater. Res.*, 2011, **391**, 1138–1142.

34 E. S. Kshumaneva, A. G. Kasikov, V. Y. Kuznetsov, Y. N. Neradovskii, R. G. Kushlyaev and V. V. Semushin, *Russ. J. Appl. Chem.*, 2015, **88**, 724–732.

35 S. Seisko, M. Lampinen, J. Aromaa, A. Laari, T. Koiranen and M. Lundström, *Miner. Eng.*, 2018, **115**, 131–141.

36 P. Altinkaya, I. Korolev, E. Kolehmainen, M. Haapalainen and M. Lundström, in *10th European Metallurgical Conference (EMC 2019)*, ed. U. Waschki, GDMB Verlag GmbH, Düsseldorf, Germany, 2019, vol. 2, pp. 821–829.

37 N. Frenzel, J. M. Hartley and G. Frisch, *Phys. Chem. Chem. Phys.*, 2017, **19**, 28841–28852.

38 G. H. Sauerbrey, *Z. Phys.*, 1959, **155**, 206–222.

39 C. K. Gupta and T. K. Mukherjee, *Hydrometallurgy in Extraction Processes*, Routledge, New York, USA, 1990, vol. 2.

40 J. J. Fritz, *J. Phys. Chem.*, 1980, **84**, 2241–2246.

41 M. Uchikoshi, *J. Solution Chem.*, 2017, **46**, 704–719.

42 M. Lampinen, S. Seisko, O. Forsström, A. Laari, J. Aromaa, M. Lundström and T. Koiranen, *Hydrometallurgy*, 2017, **169**, 103–111.

43 A. Y. M. Al-Murshedi, J. M. Hartley, A. P. Abbott and K. S. Ryder, *Trans. Inst. Met. Finish.*, 2019, **97**, 321–329.

44 D. Lloyd, T. Vainikka, L. Murtomäki, K. Kontturi and E. Ahlberg, *Electrochim. Acta*, 2011, **56**, 4942–4948.

45 J. Hartley, C.-M. Ip, G. Forrest, K. Singh, S. Gurman, K. S. Ryder, A. P. Abbott and G. Frisch, *Inorg. Chem.*, 2014, **53**, 6280–6288.

46 A. D. Ballantyne, G. C. H. Forrest, G. Frisch, J. M. Hartley and K. S. Ryder, *Phys. Chem. Chem. Phys.*, 2015, **17**, 30540–30550.

47 A. R. Hillman, *J. Solid State Electrochem.*, 2011, **15**, 1647–1660.

48 S. Kologo, M. Eyraud, L. Bonou, F. Vacandio and Y. Massiani, *Electrochim. Acta*, 2007, **52**, 3105–3113.

49 A. Collazo, R. Figueroa, X. R. Nóvoa and C. Pérez, *Surf. Coat. Technol.*, 2015, **280**, 8–15.

50 S. Bruckenstein and M. Shay, *Electrochim. Acta*, 1985, **30**, 1295–1300.

51 K. K. Kanazawa and O. R. Melroy, *IBM J. Res. Dev.*, 1993, **37**, 157–171.

52 A. R. Hillman, A. Jackson and S. J. Martin, *Anal. Chem.*, 2001, **73**, 540–549.

53 S. Ghosh, K. S. Ryder and S. Roy, *Trans. IMF*, 2014, **92**, 41–46.

54 J. G. N. Matias, J. F. Julião, D. M. Soares and A. Gorenstein, *J. Electroanal. Chem.*, 1997, **431**, 163–169.

55 J. T. Matsushima, F. Trivinho-Strixino and E. C. Pereira, *Electrochim. Acta*, 2006, **51**, 1960–1966.

56 E. Rudnik and J. Kozłowski, *Electrochim. Acta*, 2013, **107**, 103.

57 R. Schumacher, G. Borges and K. K. Kanazawa, *Surf. Sci.*, 1985, **163**, L621–L626.

58 M. Kemell, H. Saloniemi, M. Ritala and M. Leskelä, *J. Electrochem. Soc.*, 2001, **148**, C110–C118.

59 P. Redmond, A. Hallock and L. Brus, *Nano Lett.*, 2005, **5**, 131.

60 T. W. Hansen, A. T. Delariva, S. R. Challa and A. K. Datye, *Acc. Chem. Res.*, 2013, **46**, 1720–1730.

61 O. S. Hammond, H. Li, C. Westermann, A. Y. M. Al-Murshedi, F. Endres, A. P. Abbott, G. G. Warr, K. J. Edler and R. Atkin, *Nanoscale Horiz.*, 2019, **4**, 158–168.

62 J. D. Gamarra, K. Marcoen, A. Hubin and T. Hauffman, *Electrochim. Acta*, 2019, **312**, 303–312.

63 M. Iwai, H. Majima and Y. Awakura, *Hydrometallurgy*, 1988, **20**, 87–95.

64 Y. Su, J. Liu, R. Wang, S. Aisa, X. Cao, S. Li, B. Wang and Q. Zhou, *J. Electrochem. Soc.*, 2018, **165**, H78–H83.

65 T. A. Green, P. E. Valverde Armas and S. Roy, *J. Electrochem. Soc.*, 2018, **165**, D313–D320.

66 S. Dong and X. Yang, *Talanta*, 1996, **43**, 1109–1115.

67 J. J. Lingane, *Anal. Chim. Acta*, 1958, **19**, 394–401.

68 H. K. Lin, X. J. Wu and P. D. Rao, *JOM*, 1991, **43**, 60–65.

69 L. M. Abrantes, L. V. Araújo and M. D. Levi, *Miner. Eng.*, 1995, **8**, 1467–1475.

70 A. P. Abbott, K. El Ttaib, G. Frisch, K. J. McKenzie and K. S. Ryder, *Phys. Chem. Chem. Phys.*, 2009, **11**, 4269.

71 S. Ghosh and S. Roy, *Surf. Coat. Technol.*, 2014, **238**, 165–173.

72 L. N. Nekrasov, *Faraday Discuss.*, 1973, **56**, 308–316.

73 E. O. Barnes, G. E. M. Lewis, S. E. C. Dale, F. Marken and R. G. Compton, *Analyst*, 2012, **137**, 1068–1081.

74 E. Fratini, A. Girella, I. Saldan, C. Milanese, O. Dobrovetska, L. Sus, Y. Okhremchuk, O. Kuntyi and O. Reshetnyak, *Mater. Lett.*, 2015, **161**, 263–266.

75 H. E. M. Hussein, R. J. Maurer, H. Amari, J. J. P. Peters, L. Meng, R. Beanland, M. E. Newton and J. V. Macpherson, *ACS Nano*, 2018, **12**, 7388–7396.

76 E. Schalch and M. J. Nicol, *Gold Bull.*, 1978, **11**, 117–123.

77 D. J. Kinneberg, S. R. Williams and D. P. Agarwal, *Gold Bull.*, 1998, **31**, 58–67.

78 P. J. Conradie, M. W. Johns and R. J. Fowles, *Hydrometallurgy*, 1995, **37**, 349–366.

79 J. O. Marsden, *Min., Metall., Explor.*, 2006, **23**, 121–125.

80 M. Costello, in *Gold Ore Processing*, ed. M. D. Adams, Elsevier, Amsterdam, The Netherlands, 2nd edn, 2016, pp. 585–594.

81 K. Yliniemi, D. Wragg, B. P. Wilson, H. N. McMurray, D. A. Worsley, P. Schmuki and K. Kontturi, *Electrochim. Acta*, 2013, **88**, 278–286.

82 K. Yliniemi, N. T. Nguyen, S. Mohajernia, N. Liu, B. P. Wilson, P. Schmuki and M. Lundström, *J. Cleaner Prod.*, 2018, **201**, 39–48.

83 Z. Wang, P. Halli, P. Hannula, F. Liu, B. Wilson, K. Yliniemi and M. Lundström, *J. Electrochem. Soc.*, 2019, **166**, E266–E274.

84 P. Halli, B. Wilson, T. Hailemariam, P. Latostenmaa, K. Yliniemi and M. Lundström, *J. Appl. Electrochem.*, 2020, **50**, 1–14.

85 V. Miettinen, M. Haapalainen, R. Ahtiainen and J. Karonen, in *ALTA 2013 Gold Conference*, ed. A. Taylor, Perth, WA, Australia, 2013, pp. 187–202.

86 D. Lemieux, J.-M. Lalancette and B. Dubreuil, in *23rd World Mining Congress*, Canadian Institute of Mining, Metallurgy and Petroleum, Montréal, QC, Canada, 2013, p. 364.

87 E. Yazici and H. Deveci, *Int. J. Miner. Process.*, 2015, **134**, 89–96.

88 H. Elomaa, S. Seisko, T. Junnila, T. Sirviö, B. P. Wilson, J. Aromaa and M. Lundström, *Recycling*, 2017, **2**, 14.

89 Y. Ding, S. Zhang, B. Liu and B. Li, *J. Cleaner Prod.*, 2017, **165**, 48.

90 W. D. Xing, M. S. Lee and G. Senanayake, *Hydrometallurgy*, 2018, **180**, 58–64.

91 L. A. Cramer, *JOM*, 2001, **53**, 14–18.

92 F. K. Crundwell, M. S. Moats, V. Ramachandran, T. G. Robinson and W. G. Davenport, *in Extractive Metallurgy of Nickel, Cobalt and Platinum Group Metals*, Elsevier Ltd., Oxford, UK, 1st edn, 2011, pp. 489–534.

93 *CRC Handbook of Chemistry and Physics*, ed. J. R. Rumble, CRC Press, Boca Raton, FL, United States, 100th edn, 2019.

94 M. Wojnicki, K. Fitzner and M. Luty-Błocho, *Trans. Nonferrous Met. Soc. China*, 2015, **25**, 2027–2036.